

# NIR interferometry of the Seyfert galaxy NGC 1068: present interferometric results and future goals

G. Weigelt<sup>1</sup>, T. Beckert<sup>1</sup>, K.-H. Hofmann<sup>1</sup>, D. Schertl<sup>1</sup>, and M. Wittkowski<sup>2</sup>

<sup>1</sup>Max-Planck-Institut für Radioastronomie, Bonn, Germany

<sup>2</sup>European Southern Observatory, Garching, Germany

**Abstract:** We discuss present results and future goals of near-infrared interferometry of NGC 1068. We show that infrared interferometry is able to resolve the innermost, sub-parsec-scale dust environment surrounding the accretion disk. A diffraction-limited  $K'$ -band image of NGC 1068 with 74 mas resolution and the first  $H$ -band image with 57 mas resolution were reconstructed from speckle interferograms obtained with the SAO 6 m telescope. The resolved structure consists of a compact core and an extended northern and south-eastern component. The compact core has a north-western, tail-shaped extension as well as a fainter, south-eastern extension. The  $K'$ -band FWHM diameter of this compact core is approximately  $18 \times 39$  mas or  $1.3 \times 2.8$  pc, and the position angle (PA) of the north-western extension is  $-16^\circ$ . The extended northern component (PA  $\sim 0^\circ$ ) has an elongated structure with a length of about 400 mas or 29 pc. The PA of  $-16^\circ$  of the compact  $18 \times 39$  mas core is very similar to that of the western wall (PA  $\sim -15^\circ$ ) of the ionization cone. This suggests that the  $H$ - and  $K'$ -band emission from the compact core is both thermal emission and scattered light from dust near the western wall of a low-density, conical outflow cavity or from the innermost region of a parsec-scale dusty torus that is heated by the central source (the dust sublimation radius of NGC 1068 is approximately 0.1 – 1 pc). The first near-infrared  $K$ -band long-baseline interferometry of the nucleus of NGC 1068 with resolution  $\lambda/B \sim 10$  mas was obtained with the ESO VLTI. A squared visibility amplitude of  $16.3 \pm 4.3\%$  was measured for NGC 1068 at a sky-projected baseline length of 45.8 m. Taking into account  $K$ -band speckle interferometry observations, the VLTI observations suggest a multi-component structure for the intensity distribution, where part of the flux originates from scales clearly smaller than  $\sim 5$  mas ( $\lesssim 0.4$  pc).

## 1 Bispectrum speckle interferometry of the Seyfert 2 galaxy NGC 1068

### 1.1 Speckle Interferometry Visibilities

Figures 1 and 2 show all two-dimensional  $K'$ - and  $H$ -band visibility functions of NGC 1068 obtained with the SAO 6 m telescope at four epochs between 1997 and 2003 (Weigelt et al. 2004) as well as the  $K$ -band visibilities reconstructed from the 1996 data (Wittkowski et al. 1998), cuts through the two-dimensional visibilities along the major and minor axes, and cuts through the model fits of

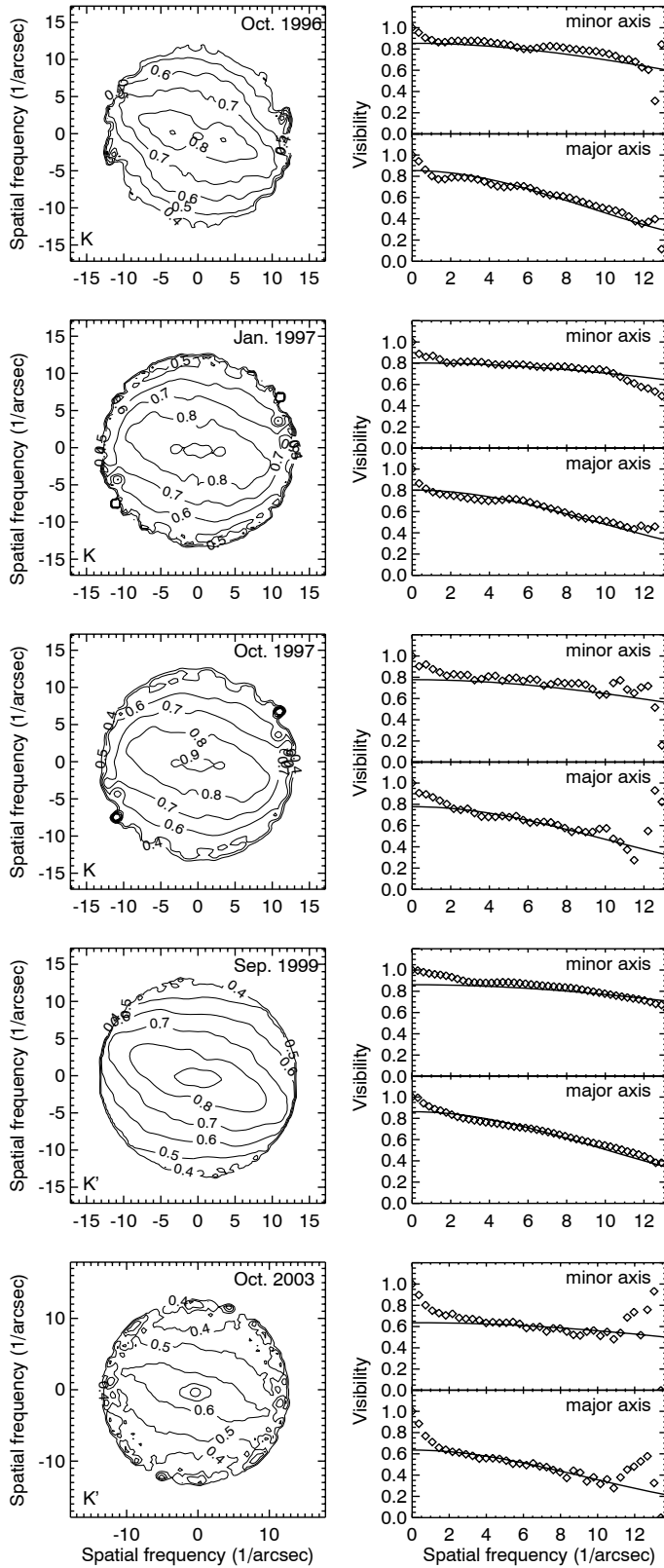


Figure 1: **Left:**  $K$ - or  $K'$ -band visibilities of NGC 1068 observed in 1996, 1997, 1999, and 2003. **Right:** Cuts through their major and minor axes. North is at the top and east to the left in the corresponding image. The contours are spaced from 40 to 90% in 6 steps. The diamonds are observations, and the solid lines are cuts through fits of two-dimensional Gaussian brightness distributions (fit range 30 to 80% of the telescope cut-off frequency).

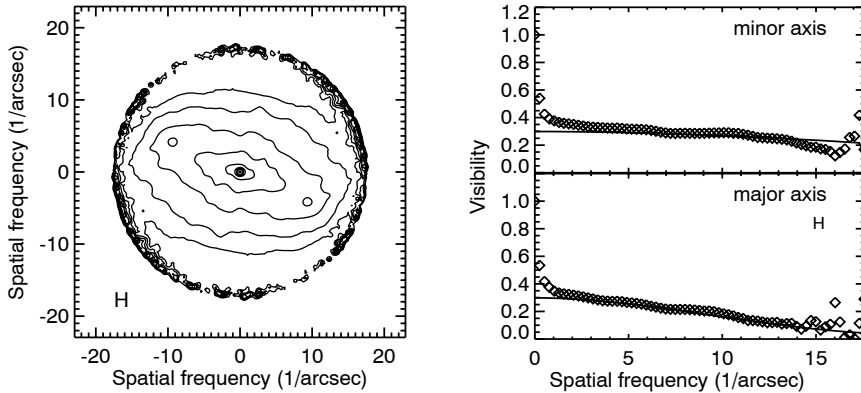


Figure 2: Two-dimensional  $H$ -band visibilities of NGC 1068 and cuts through their major and minor axes. The contours are spaced from 10 to 90% in 18 linear steps. Diamonds are observations, solid lines are fits of a two-dimensional Gaussian brightness distribution.

two-dimensional elliptical Gaussian brightness distributions. All visibilities show similar, elongated shapes. The low-frequency peak of all visibility functions at spatial frequencies of up to  $\sim 2 \text{ arcsec}^{-1}$  is caused by the host galaxy and an additional extended component.

The shapes of all visibility functions show that the dominant compact core of NGC 1068 is elongated. We have derived the size of this resolved compact core of NGC 1068 by fitting a single-component elliptical Gaussian brightness distribution (a two-component model fit is discussed below) to the data in the range of 30 to 80% of the telescope cut-off frequency. The  $K'$ - and  $H$ -band telescope cut-off frequencies are at spatial frequencies of approximately 13 and 17  $\text{arcsec}^{-1}$ , respectively. This fit range excludes both the low-frequency peak (host galaxy and extended component) and the less accurate highest spatial frequencies.

We obtained an average  $K'$  diameter (FWHM, Gaussian fit) of  $18.4 \times 39.4 \text{ mas}$  and a PA of  $-16^\circ$  (for the long axis in image space). In the following text we call this resolved compact core, which has a similar but not identical size in the  $H$  band, simply the  $18 \times 39 \text{ mas}$  object or component.

The FWHM  $H$ -band diameters of the minor and major axes of the compact component are 18.4 and 44.7 mas, respectively, and the PA is  $-18^\circ$ . The total error of the derived  $K'$ - and  $H$ -band sizes is  $\pm 4 \text{ mas}$ , and the error of the position angles is  $\pm 4^\circ$ .

Finally, we studied how the size of the compact  $K'$ -band component changes if we fit a two-component model to the visibilities. The two-component model consists of a two-dimensional elliptical Gaussian intensity contributing 60% of the flux plus a point source contributing 40%. With this model we derived a larger FWHM diameter of  $26 \times 58 \text{ mas}$  for the compact component.

## 1.2 Bispectrum speckle interferometry: images of the $1.3 \times 2.8 \text{ pc}$ core

Diffraction-limited  $K$ - and  $K'$ -band images with 74 – 76 mas resolution and an  $H$ -band image with 57 mas resolution (see Fig. 3) were reconstructed from speckle interferograms obtained with the SAO 6 m telescope using bispectrum speckle interferometry (see Wittkowski et al. 1998 and Weigelt et al. 2004 for more details). The resolved structure consists of a compact core and an extended northern and south-eastern component. The compact core has a north-western, tail-shaped extension as well as a fainter, south-eastern extension. The  $K'$ -band FWHM diameter of this resolved compact core is  $\sim 18 \times 39 \text{ mas}$  or  $1.3 \times 2.8 \text{ pc}$ , as discussed already in the previous section. The position angle of the north-western extension is  $-16 \pm 4^\circ$ . The extended northern component (PA  $\sim 0^\circ$ ) has an elongated structure with a length of about 400 mas or 29 pc.

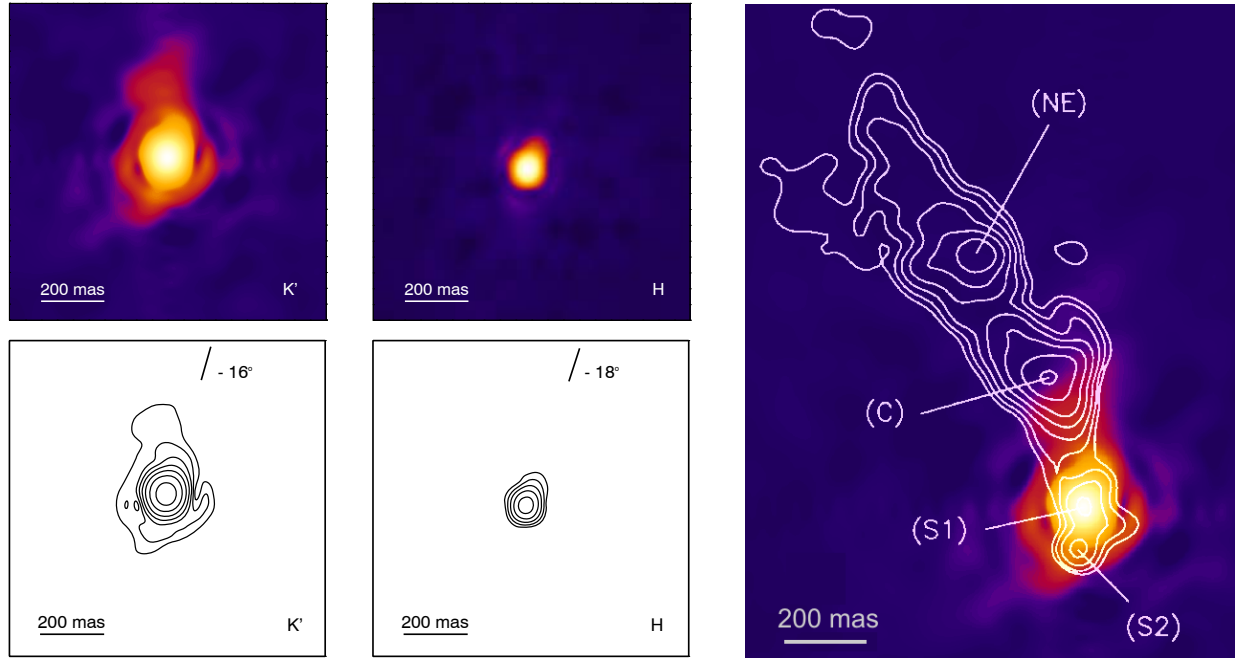


Figure 3: **Left, top, and bottom:** Diffraction-limited  $K'$ -band image of NGC 1068 reconstructed by bispectrum speckle interferometry. The image shows the compact core (yellow) with its tail-shaped, north-western extension at a PA of  $\sim -16^\circ$  as well as the northern and south-eastern extended components (red). In addition to these structures, the first diffraction ring around the compact component is visible. North is up, and east is to the left. **Middle, top, and bottom:** Diffraction-limited  $H$ -band image, which also shows the tail-shaped, north-western extension. **Right:** MERLIN 5 GHz contour map (Gallimore et al. 1996) superposed on our  $K'$  image. The center of the radio component S1 coincides with the center of the  $K'$  peak. The PA of  $-16^\circ$  of the  $18 \times 39$  mas  $K'$ -band core is very similar to that of the western wall (PA  $\sim -15^\circ$ ) of the bright region of the ionization cone. The northern extended 400 mas structure (red) aligns with the direction of the inner radio jet (S1 – C). The northern borderline of the northern component is almost perpendicular to the radio jet between C and NE. The PA of the south-eastern extended component is similar to the PA of S1 – S2.

The PA of  $-16 \pm 4^\circ$  of the compact  $18 \times 39$  mas core is very similar to that of the western wall (PA  $\sim -15^\circ$ ) of the bright region of the ionization cone. This suggests that the  $H$ - and  $K'$ -band emission from the compact core is both thermal emission and scattered light from dust near the western wall of a low-density, conical cavity or from the innermost region of a parsec-scale dusty torus heated by the central source (the dust sublimation radius of NGC 1068 is approximately 0.1 – 1 pc; see references in Weigelt et al. 2004). The northern extended 400 mas structure lies near the western wall of the ionization cone and coincides with the inner radio jet (PA  $\sim 11^\circ$ ). The large distance from the core suggests that the  $K'$ -band emission of the northern extended component is scattered light from the western cavity region and the radio jet region.

### 1.3 Interpretation

Emission in the  $K'$  band can be interpreted as scattered and direct thermal radiation of hot dust near its sublimation temperature ( $\sim 1000 - 1500$  K), located at the inner edge of the dusty torus or in the polar cone between the broad and narrow line region. Depending on the chemical composition and optical properties of the dust, the sublimation radius is estimated to be 0.1–1 pc (see Weigelt et

al. 2004 for more details). In addition to the unknown dust properties, the luminosity of the central source is also uncertain, and estimates range from  $2 \cdot 10^{11}$  to  $2.5 \cdot 10^{12} L_{\odot}$  (e.g., Bock et al. 2000, Marco & Alloin 2000). The major axis of the resolved core points to the western wall of the ionization cone, and the extension in this direction is expected to be larger than the sublimation diameter (see Fig. 5).

For a quantitative analysis of the  $K'$ -band flux emerging from an optically thick torus, accurate radiative transfer modeling is necessary. A number of models have been published for NGC 1068 (Pier & Krolik 1992, 1993, Granato & Danese 1994, Efstathiou & Rowan-Robinson 1995, Efstathiou et al. 1995, Granato et al. 1997, Manske et al. 1998, Nenkova et al. 2002, Galliano et al. 2003). All these models try to fit the SED of Rieke & Low (1975) with a  $K$ -band flux of  $0.3 \pm 0.1$  Jy. Torus models which can explain the observed infrared SED by emission exclusively from the torus (i.e., without dust within the ionization cone) were presented by Granato & Danese (1994). But as pointed out in a recent discussion by Galliano et al. (2003), various models with different combinations of parameters are consistent with the nuclear SED.

Due to the proposed clumpiness of the torus (Krolik & Begelman 1988, Nenkova et al. 2002, Vollmer et al. 2004) there is a possibility that a fraction of the flux of the central source reaches us directly without being strongly absorbed or scattered. Therefore, a non-negligible contribution at  $2 \mu\text{m}$  may come from an optically thick, geometrically thin standard accretion disk surrounding the central engine or from the high-frequency tail of synchrotron emission of the radio component S1 if it is actually optically thin synchrotron radiation (Beckert & Duschl 1997, Wittkowski et al. 1998).

## 2 VLTI long-baseline interferometry of NGC 1068

The ESO Very Large Telescope Interferometer with its AMBER phase-closure instrument will provide the spectacular resolution of 2 mas at the wavelength of 1 micron. The high-precision determination of small differences between visibilities at different wavelengths achievable with AMBER will very likely allow even the resolution of the Broad-Line Region of AGN in the infrared.

The first near-infrared  $K$ -band long-baseline interferometry of the nucleus of NGC 1068 with resolution  $\lambda/B \sim 10$  mas was obtained with the Very Large Telescope Interferometer (VLTI; two 8.2 m diameter telescopes UT 2 and UT 3; Wittkowski et al. 2004). The adaptive optics system MACAO was employed to deliver wavefront-corrected beams to the  $K$ -band instrument VINCI. A squared visibility amplitude of  $16.3 \pm 4.3$  % was measured for NGC 1068 at a sky-projected baseline length of 45.8 m. This value corresponds to a FWHM size of the observed  $K$ -band structure of  $5.0 \pm 0.5$  mas ( $0.4 \pm 0.04$  pc) if it consists of a single Gaussian component. Taking into account  $K$ -band speckle interferometry observations (Wittkowski et al. 1998, Weinberger et al. 1999, Weigelt et al. 2004), these observations suggest a multi-component structure for the intensity distribution, where one part of the flux originates from scales clearly smaller than  $\sim 5$  mas ( $\lesssim 0.4$  pc) and another part from larger scales. The  $K$ -band emission from the small ( $\lesssim 5$  mas) scales might arise from the substructure of the dusty torus or directly from the central accretion flow viewed through only moderate extinction (see Wittkowski et al. 2004 for more details).

## 3 Clumpy torus model

To explain the torus substructure in NGC 1068 mentioned above, the existence of cold and dusty clouds in a geometrically thick torus with only a few clouds along the line of sight is required. We have applied the radiative transfer treatment in a clumpy medium (Nenkova et al. 2002) to our dynamical model of clouds in the torus of NGC 1068 (Beckert & Duschl 2004). The resulting model image (Fig. 6) allows a comparison with the structures (size, shape, and flux) seen in Fig. 3.

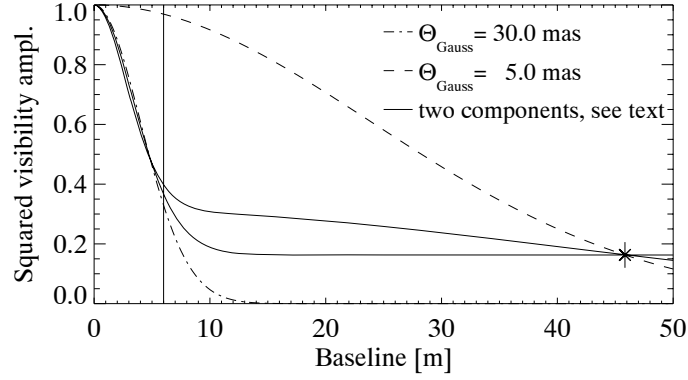


Figure 4: Synthetic squared visibility function for a 5 mas (dashed line) Gaussian, a 30 mas (dashed-dotted line) Gaussian, and two examples (solid lines) of a two-component model where (upper line/lower line) 56%/40% of the total flux comes from a 3 mas/0.1 mas Gaussian and the remaining 44%/60% from a 54 mas/42 mas Gaussian (FWHM). Measurements are available for baselines  $B = 46$  m and up to  $B = 6$  m as discussed above. Both measurements are only matched if the small component has a size clearly below  $\sim 5$  mas and if only part of the total flux in our FOV arises from this  $\lesssim 5$  mas component and another part from a larger structure.

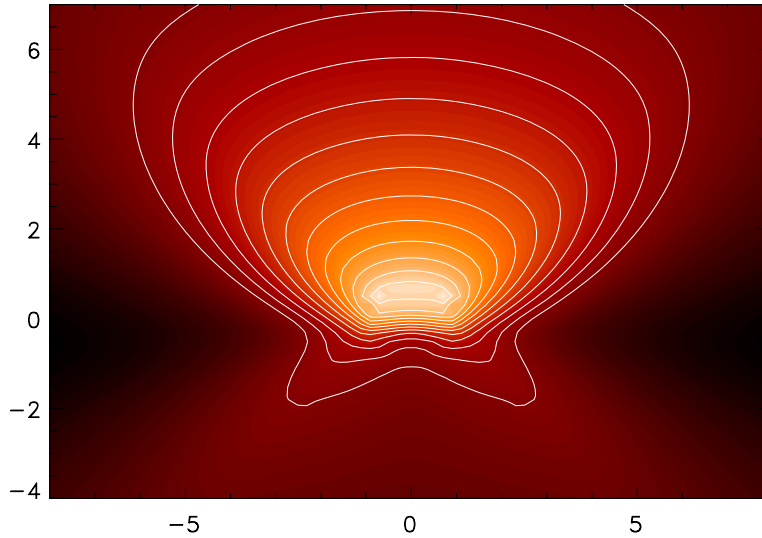


Figure 5:  $K$ -band surface brightness of a clumpy torus model for an inclination of  $60^\circ$ . The dynamic range of the contour levels is  $2^{12}$ . The linear scale of the image is in units of the dust sublimation radius ( $\sim 1$  pc). The brightest region is the illuminated inner wall on the opposite side of the torus.

## 4 Future goals

High-resolution near-infrared observations of AGN will test present unification schemes, which predict the presence of clumpy, dusty tori emitting reprocessed radiation from the NIR to the FIR. Furthermore, physical properties of outflows and jets and the connection between AGN and circumnuclear starburst activity can be studied in greater detail. These studies will improve our understanding of the fueling of black holes via accretion through nuclear disks and dusty tori. It will be possible to investigate, through a combination of interferometric observations and theoretical studies, how accretion processes at different length scales work and how they relate to each other.

The interferometric results will show whether the theoretical torus models are viable and what kind of additional extended structures can be seen and have to be accounted for in the models. Together with an understanding of the post-merger evolution of the large-scale ISM and associated starburst activity in the host galaxy, unique information on properties of the gas and dust available for fueling the growth of the black holes can be derived. As shown by the observations of the torus in NGC 1068, it will be possible to explore the internal structure of tori around AGN. This will provide information on dynamical processes between clouds in the torus, the resulting transport of matter, and fueling of the black hole accretion disk.

For example, the near-infrared beam combiner instrument AMBER for the VLTI can contribute to these projects due to its high spatial resolution of 4 mas at  $2\ \mu\text{m}$  and 100 m baseline and its spectroscopic capabilities (spectral resolution between 30 and 10 000). The expected limiting K-band magnitude of AMBER is approximately 13 mag. AMBER will allow us to carry out phase-closure measurements with three 8 m telescopes and to reconstruct images with unprecedented angular resolution.

In the future, interferometer baseline lengths of up to 1 km will be required since the 100 m baseline of the VLTI UT array only allows a partial resolution of the fine structure of AGN tori and of the BLR of a few favorable objects. Furthermore, a large number of 8 m telescopes (at least 6) are required in order to obtain good uv coverage and to be able to reconstruct precise images.

## References

- Beckert T., Duschl W. J., 1997, A&A 328, 95  
Beckert T., Duschl W. J., 2004, A&A 426, 445  
Bock J. J., Neugebauer G., Matthews K., et al., 2000, AJ 120, 2904  
Efstathiou A., Rowan-Robinson M., 1995, MNRAS 273, 649  
Efstathiou A., Hough J. H., Young S., 1995, MNRAS 277, 1134  
Galliano E., Alloin D., Granato G. L., Villar-Martin M., 2003, A&A 412, 615  
Gallimore J. F., Baum S. A., O’Dea, C. P., 1996, ApJ 464, 198  
Granato G. L., Danese L., 1994, MNRAS 268, 235  
Granato G. L., Danese L., Franceschini A., 1997, ApJ 486, 147  
Krolik J. H., Begelman M. C., 1988, ApJ 329, 702  
Manske V., Henning Th., Men’shchikov A. B., 1998, A&A 331, 52  
Marco O., Alloin D., 2000, A&A 353, 465  
Nenkova M., Ivezić Z., Elitzur M., 2002, ApJ 570, L9  
Pier E. A., Krolik J. H., 1992, ApJ 401, 99  
Pier E. A., Krolik J. H., 1992, ApJ 418, 673  
Rieke G. H., Low F. J., 1975, ApJ 199, L13  
Vollmer B., Beckert T., Duschl W. J., 2004, A&A 413, 949  
Weigelt G., Wittkowski M., Balega Y. Y., et al., 2004, A&A 425, 77  
Weinberger A. J., Neugebauer G., Matthews K., 1999, AJ 117, 2748

- Wittkowski M., Balega Y., Beckert T., Duschl W. J., Hofmann K.-H., Weigelt G., 1998, A&A 329, L45
- Wittkowski M., Kervella P., Arsenault R., Paresce F., Beckert T., Weigelt G., 2004, A&A 418, L39